Annihilation rate in positronic systems by quantum Monte Carlo: e^+LiH as test case

Massimo Mella[a] and Simone Chiesa[b]
Dipartimento di Chimica Fisica ed Elettrochimica, Universitá degli Studi di Milano, via Golgi 19, 20133 Milano, Italy

Gabriele Morosi[c]
Dipartimento di Scienze Chimiche, Fisiche e Matematiche, Universitá dell'Insubria, via Lucini 3, 22100 Como, Italy

An accurate method to compute the annihilation rate in positronic systems by means of quantum Monte Carlo simulations is tested and compared with previously proposed methods using simple model systems. This method can be applied within all the quantum Monte Carlo techniques, just requiring the accumulation of the positron–electron distribution function. The annihilation rate of e^+LiH as a function of the internuclear distance is studied using a model potential approach to eliminate the core electrons of Li, and explicitly correlated wave functions to deal with all the remaining particles. These results allow us to compute vibrationally averaged annihilation rates, and to understand the effect of the Li^+ electric field on positron and electron distributions. © *2002 American Institute of Physics.* [DOI: 10.1063/1.1436464]

I. INTRODUCTION

In positron and positronium (Ps) chemistry and physics, the annihilation rate $\Gamma_{2\gamma}$ plays an important role since it correlates with many aspects of the local environment where the positron annihilates. For instance, "pick-off" annihilation in solutions and in solid materials, "on the fly" annihilation in atomic and molecular gases, and bound state annihilation of positronic compounds are just few of the experiments where $\Gamma_{2\gamma}$ can be measured and successively interpreted.

Although these experiments are relevant both technologically and scientifically,[1,2] only few theoretical studies have been devoted to accurately compute annihilation rates for realistic systems like atoms and molecules in order to compare with experimental data or to predict trends.[3–11] Moreover, these have been restricted to deal with at most four active electrons, so that only a bunch of systems have been studied so far. We believe this scarceness of results to be primarily due to the intrinsic difficulty in obtaining accurate wave functions for larger systems, and to the computational effort requested with respect to ordinary matter compounds when standard *ab initio* methods are employed.[12]

For these reasons, quantum Monte Carlo (QMC) methods[13] represent an alluring alternative to these methods, to density functional theory, and to explicitly correlated wave functions in computing energies and properties of realistic positronic systems. QMC techniques are well described in the literature, so we avoid burdening this paper with the details of the methods and constrain ourselves to discuss only the technical issues relevant for the specific problem.

Not requiring the analytical calculation of integrals, QMC allows one to use any physically sensible wave function. This possibility increases the chances to obtain an accurate description of any class of systems once all the relevant physical information is included in the chosen analytical form of the wave function. Having defined a trial wave function Ψ_T for a system, QMC techniques allow one to compute the differential and nondifferential properties of the system by sampling Ψ_T^2, $\Psi_T\Psi_0$, or Ψ_0^2. Here, Ψ_0 is the exact ground-state function of the system. This task is usually accomplished by creating a distribution of points (also known as configurations or walkers) in configurational space whose density is proportional to the aforementioned Ψ_T^2, $\Psi_T\Psi_0$, or Ψ_0^2.

Keeping in mind the above remarks, it might appear that the QMC methods should accurately predict any interesting observable for positronic systems. This is indeed correct except for extremely local operators like Dirac's delta (δ), and hence for $\Gamma_{2\gamma}$ which is proportional to its expectation value, for which an accurate sampling of small configurational space volumes is needed. These operators are well known to represent a challenge for QMC due to the discrete nature of the configuration ensemble and the finite length of the simulations.

As far as the mean value of the Dirac's delta (δ) operator is concerned, one faces an additional difficulty when trying to estimate its mean value. Even admitting a perfect sampling in the regions where two particles are close to each other, the primitive method of counting the number of times the interparticle distance r is smaller than a given radius r_w (i.e., counting the ones that fall into a spherical well of radius r_w)[5] has an associated statistical error that diverges for $r_w \rightarrow 0$.[11] This fact means that the estimation of the statistical error of the extrapolated value is based on shaky grounds.

[a]Electronic mail: Massimo.Mella@unimi.it
[b]Electronic mail: Simone.Chiesa@unimi.it
[c]Electronic mail: Gabriele.Morosi@uninsubria.it

J. Chem. Phys., Vol. 116, No. 7, 15 February 2002

Positronic systems   2853

Although not a solution, a slightly better approach was devised by substituting the simple sphere with a Gaussian function centered at the coalescence point.[8,9,11] The variance of this estimator also goes to infinity upon decreasing of the Gaussian width, but it diverges less fast than the one of the spherical well, therefore allowing a statistically more accurate estimation of $\langle \delta(r_{-+}) \rangle = \Sigma_i \langle \delta(r_{i+}) \rangle$.

Due to the interest in computing $\langle \delta(r) \rangle$ for many systems, efforts have been made to solve these problems, and remedies have been suggested in the framework of all the QMC techniques.

As far as variational Monte Carlo (VMC) is concerned, different methods have been proposed that may solve this difficulty, allowing one to compute the needed quantities. One of these methods starts from the distribution differential identity

$$\nabla^2 \frac{1}{r} = -4\pi \delta(r), \tag{1}$$

which allows one to write, after specializing for the electron–positron pair[10]

$$\langle \delta(r_{1+}) \rangle_T = \int \delta(r_{1+}) \Psi_T^2(\mathbf{R}) d\mathbf{R}$$

$$= -\frac{1}{2\pi} \int \Psi_T^2(\mathbf{R})$$

$$\times \left\{ \frac{\nabla_{\mathbf{r}_1}^2 \Psi_T(\mathbf{R})}{\Psi_T(\mathbf{R})} + [\nabla_{\mathbf{r}_1} \ln \Psi_T(\mathbf{R})]^2 \right\} \frac{1}{r_{1+}} d\mathbf{R}, \tag{2}$$

where $\mathbf{R} = (\mathbf{r}_1, \mathbf{r}_2, \ldots, \mathbf{r}_+)$ is a point in configuration space, and the trial wave function Ψ_T is normalized. Although this integral has a well-defined value that can be computed sampling Ψ_T^2, it is well known that its variance diverges over the same distribution.[14] This fact implies that no error bound (i.e., standard deviation) can be associated with its value, a dangerous situation one would like to avoid.

Langfelder et al.[14] proposed a possible way to circumvent this problem based on a modified importance sampling transformation, where $\Psi_T^2 \Sigma_i 1/r_{i+}^2$ is sampled instead of Ψ_T^2.

Always starting from Eq. (2), one could also exploit the approach proposed by Assaraf and Caffarel[15] to compute the expectation value needed to obtain nuclear forces by means of the Hellman–Feynmann theorem. They showed that a judicious choice of a renormalized operator, whose mean value is equal to the original one, can reduce the infinite variance to a finite value.[16]

A completely different approach was pursued by Alexander and Coldwell.[17] They proposed to compute all the mean values sampling an analytically normalizable distribution function $g(\mathbf{R})$, so that the normalization N_T of Ψ_T is easily estimated by means of

$$\frac{1}{N_T^2} = M^{-1} \sum_{i=1}^{M} \Psi_T^2(\mathbf{R}_i)/g(\mathbf{R}_i), \tag{3}$$

where the M points sample the normalized g. If a second normalizable distribution $g_c(\mathbf{R})$, constrained on the subspace $\mathbf{r}_+ = \mathbf{r}_1$, is employed to guide the simulation and to compute N_T^c in Eq. (3), then $\langle \delta(r_{-+}) \rangle$ can be easily estimated by the $(N_T^c/N_T)^2$ ratio.

Although these three methods represent a step towards the solution of this complicated problem in the VMC framework, and are currently used for ordinary electronic compounds with success, the situation still remains far from satisfactory for positronic systems. For these systems beyond the problem of the method used to compute $\langle \delta \rangle$, there is another difficulty: as far as we know, nobody has been able to optimize an accurate Ψ_T for a positronic system with more than four electrons. More specifically, for large systems explicit correlation between the electrons and the positron has been difficult to introduce.[11] This means that the "pileup" of the electron density over the positron is not correctly described, therefore giving rise to annihilation rates that are too small.[18] Possible sources of this unwanted outcome are the lack of knowledge about the complicated analytical form that such an accurate wave function should have, and some drawbacks of the optimization method used.[19]

In order to go beyond these difficulties, the diffusion Monte Carlo (DMC) method is usually employed to sample $\Psi_T \Psi_0$.[20–22] This technique is able to project the contribution of the excited states from the starting Ψ_T, allowing the exact calculation of the ground-state energy. Unfortunately, the $\delta(r_{-+})$ operator does not commute with the Hamiltonian of the system, so the simulation results are only an approximation to the exact mean value when computed by means of the mixed estimator

$$\langle \delta(\mathbf{r}_{-+}) \rangle_M = \int \delta(r_{-+}) \Psi_T \Psi_0 d\mathbf{R}. \tag{4}$$

Although this value represents a more accurate estimate of the exact $\langle \delta(r_{-+}) \rangle$ than $\langle \delta(r_{-+}) \rangle_T$, it has been found that the quality of the results strongly depends on how accurately Ψ_T mimics the correct interparticle distributions.

Whereas both the spherical well and Gaussian method can be employed to estimate $\langle \delta(r_{-+}) \rangle_M$ in Eq. (4), Jiang and Schrader[5] pointed out that the use of the differential identity Eq. (1) in a DMC simulation requires some uncontrolled approximation, since $\Psi_T \Psi_0$ is not known analytically but only sampled.

Nevertheless, it has been shown[10] that an accurate estimate of $\langle \delta(r_{-+}) \rangle$ can be obtained simply by substituting Ψ_T^2 in Eq. (2) with $\Psi_T \Psi_0$, if Ψ_T correctly describes the positron–electron distribution.

A possible solution to the difficulty that DMC meets in estimating the exact expectation values is represented by sampling Ψ_0^2 instead of $\Psi_T \Psi_0$, and computing $\langle \delta(r_{-+}) \rangle$ without resorting to Ψ_T in any way. This idea rules out the possibility of using Eq. (1), since one just samples the exact Ψ_0^2 distribution and no analytical information is available about its form.

In order to overcome this problem, Langfelder et al.[14] proposed to correct $\langle \delta(r) \rangle_T$ by accumulating the walker weights in a small sphere around the coalescence point. Although this way may look promising, we noticed in our work on positron complexes[23] that long decaying times are needed in order to project all the excited-state contributions and to

correctly build the pileup of the electron density over the positron if Ψ_T poorly describes this feature. This fact produces large fluctuations in the weight values, therefore increasing the statistical noise of the results.

A better approach may be represented by the use of the tagging algorithm proposed by Barnett *et al.*[24] in connection with the branching step usually employed in DMC. Here, the ratio Ψ_0/Ψ_T, needed to sample Ψ_0^2, is computed by means of the number of daughters of each configuration.

Moreover, Baroni and Moroni[25] have recently proposed an alternative algorithm that appears to be well suited for this task. This is based on a ''path integral'' view of the DMC algorithm, where the branching step has been substituted by an accept/reject step in order to exactly sample Ψ_0^2.

Unfortunately, these approaches do not solve the problem of the scarce sampling in the volume around $r=0$, a problem that is present even for small simulation time steps. As stated previously, this comes from the finite length and discrete nature of the QMC simulations. As an attempt to overcome this difficulty, Langfelder *et al.*[14] implemented in their algorithm the correct sampling of the electron–nucleus cusp region as proposed by Umrigar *et al.*:[26] this adaptation, however, does not appear straightforward to correct the sampling of both the electron–electron and electron–positron cusps.

Keeping in mind all the aforementioned problems in estimating $\langle\delta\rangle$, we believe the Monte Carlo practitioners are left only with the hope of devising an approximate, but hopefully solid and accurate, method to compute this observable.

The main aim of this paper is to discuss and test the accuracy of computing $\langle\delta\rangle$ using some simple methods based only on the sampling of the positron–electron distribution function without any usage of the differential identity Eq. (1). These methods will be compared with the Gaussian approximation discussing relative merits and applicability. Moreover, we apply them to the realistic e^+LiH model case in order to study the annihilation rate as a function of the internuclear distance R. The $\Gamma_{2\gamma}$ versus R results will allow us to compute the vibrationally averaged annihilation rate for this system and to discuss molecular environment effects on the annihilation rate itself and on contact distribution functions.

The outline of this work follows. In Sec. II we present the basis of the methods. Section III describes their applications to model systems for which the exact $\langle\delta\rangle$'s are known. As an application of this technique, we deal in Sec. IV with the model e^+LiH. Our conclusions and proposals for future work are then presented in Sec. V.

II. METHODS

Since we want to develop a method that can be applied to any QMC technique, henceforth we will use $f(\mathbf{R})$ to indicate cumulatively $\Psi_T^2(\mathbf{R})$, $\Psi_T(\mathbf{R})\Psi_0(\mathbf{R})$, or $\Psi_0^2(\mathbf{R})$. Here, $\mathbf{R}=(\mathbf{r}_1,\mathbf{r}_2,\dots,\mathbf{r}_+)$ is a point in configuration space, $\mathbf{r}_i$ and $\mathbf{r}_+$ being, respectively, the ith electron and positron positions.

We are interested in computing the expectation value $\langle\delta(r_{-+})\rangle$ over the distribution $f(\mathbf{R})$, i.e.,
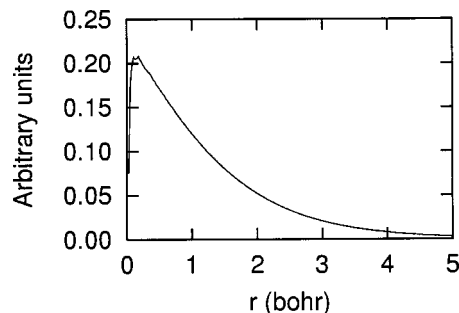

FIG. 1. Behavior of $\Omega(r_{-+})$ sampled from Ψ_1.

$$\langle\delta(r_{-+})\rangle=\frac{\int f(\mathbf{R})\delta(r_{-+})d\mathbf{R}}{\int f(\mathbf{R})d\mathbf{R}}. \quad (5)$$

Recalling that $f(\mathbf{R})$ is symmetric under any exchange between electrons, Eq. (5) can be rewritten as

$$\langle\delta(r_{-+})\rangle=\frac{\int\rho(\mathbf{r}_-,\mathbf{r}_+)\delta(r_{-+})d\mathbf{r}_-\,d\mathbf{r}_+}{\int\rho(\mathbf{r}_-,\mathbf{r}_+)d\mathbf{r}_-\,d\mathbf{r}_+}, \quad (6)$$

where $\rho(\mathbf{r}_-,\mathbf{r}_+)=N_{ele}\int f(\mathbf{R})d\mathbf{r}_2,\dots,d\mathbf{r}_N$. Introducing the new coordinates $\mathbf{R}_{-+}=\mathbf{r}_-+\mathbf{r}_+$ and $\mathbf{r}_{-+}=\mathbf{r}_+-\mathbf{r}_-$, after integration over $\mathbf{R}_{-+}$ and spherically averaging over $\mathbf{r}_{-+}$, one gets

$$\begin{aligned}\langle\delta(r_{-+})\rangle&=\frac{\int\Omega(\mathbf{r}_{-+})\delta(r_{-+})d\mathbf{r}_{-+}}{\int\Omega(\mathbf{r}_{-+})d\mathbf{r}_{-+}}\\&=\frac{\int\Omega(\mathbf{r}_{-+})\delta(r_{-+})r_{-+}^2\,dr_{-+}}{\int\Omega(r_{-+})r_{-+}^2\,dr_{-+}}\\&=\frac{\Omega(0)}{\int\Omega(r_{-+})r_{-+}^2\,dr_{-+}},\end{aligned} \quad (7)$$

where $\Omega(r_{-+})$ is the spherically averaged positron–electron distribution. Although these manipulations are quite straightforward, they highlight that in order to compute $\langle\delta(r_{-+})\rangle$ one must have accurate values for both $\Omega(0)$ and the denominator $\int\Omega(r_{-+})r_{-+}^2\,dr_{-+}$. Therefore, both the coalescence region and the tail of the distribution must be correctly described.

In order to thoroughly present the complexity of the current problem, Fig. 1 shows a typical behavior of $\Omega(r_{-+})$ as sampled from the model wave function for one electron and one positron

$$\Psi_1(\mathbf{r}_-,\mathbf{r}_+)=\exp[-r_--0.25r_+-0.25r_{-+}], \quad (8)$$

by means of a standard VMC simulation using the Langevin algorithm and the accept/reject step.[13] This simulation was carried out sampling a grand total of 3.75×10^9 configurations and using a time step of 0.01 hartree^{-1}, a fairly small time step for this simple wave function. The sampled distribution of $r_{-+}=r$ was collected on a grid with a bin width of $\delta r=0.025$ bohr, and then the number of times r_{-+} was found inside a given bin was divided by the volume of the spherical crown $[r-\delta r,r]$, $V(r,\delta r)=4\pi/3[3r^2\delta r-3r\delta r^2+\delta r^3]$. The values so obtained were attributed to the mean radius of the spherical crown, $\bar r=\pi\delta r[4r^3-6r^2\delta r+4r\delta r^2$

$-\delta r^3]/V(r,\delta r)$. This is equivalent to approximating $\Omega(r)$ as a straight line inside each spherical crown, a fairly good approximation in such a small bin.

We want to stress that the shape of the distribution was found independent of the time step over a broad range of values. This ensures that no systematic bias is present due to the finite time step. From Fig. 1 one can easily notice the abrupt decrease of the distribution in the region close to $r=0$. This represents the aforementioned inability of Monte Carlo simulations to correctly sample the distribution close to a coalescence point in spite of the large number of sampled configurations. It also seems to indicate that, due to this inability, any well-based method (e.g., both the spherical well and Gaussian methods) should return an inaccurate answer for r_w smaller than a certain threshold. Conversely, all the regions with $r>0.5$ bohr seem to be adequately described by the sampled distribution, and therefore we propose to analytically continue their shape extrapolating to $r=0$ by means of a suitable functional form. This idea allows one to exploit the knowledge about the exact form of Ω to improve the local description in the small radius regions. For instance, if one samples $f=\Psi_0^2$, the exact value of the cusp condition can be used as a way to constrain the model to behave correctly. This trick can also be used in both the VMC and DMC simulations, since it is often easy to obtain the cusp condition of the sampled f knowing the analytical form of Ψ_T. This method could be implemented in two different ways. First, one could choose an analytical function $\omega(r)$ to fit Ω for all the electron–positron distances. This function should be flexible enough to properly describe both short-range and long-range behavior of Ω. More specifically, close to $r=0$ $\Omega(r)$ behaves like $\exp(-\alpha r)$, where α is strictly related to the cusp condition. Differently, in the large r regions $\Omega(r)$ follows $\exp(-\beta r)$, where β is dependent on the positron affinity (PA) of the system. A possible choice for $\omega(r)$ is the Padé–Jastrow form

$$\omega(r)=N_\omega \exp\left[-\frac{\alpha r+\beta r^2}{1+\gamma r}\right], \qquad (9)$$

where α can be chosen to have $\omega(r)$ satisfy the correct local behavior close to $r=0$. The fitted form can successively be used to estimate both $\Omega(0)$ and the denominator in Eq. (7).

Second, if the form of $\Omega(r)$ is more complicated (e.g., it has multiple maxima), it is possible to resort to a local fit by $\omega(r)$ in the region close to the cusp in order to get the $\Omega(0)$ value. Then, the normalization integral could be split in two parts, one computed using $\omega(r)$ and the other directly using the sampled distribution. Specifically for the distribution in Fig. 1, one could fit the sampled Ω values in the range [0.5, 1.0] bohr constraining $\omega(r)$ to have both the exact cusp behavior and to have the same value of the sampled Ω for $r=1.0$ bohr. Then, the normalization integral can be estimated integrating numerically $\omega(r)$ for $0\leq r\leq1.0$, and employing the trapezoidal formula for the remaining sampled values. We would like to mention that this necessity is already present for small systems like e^+Be.[27]

Although the two proposed methods are approximate, they might prove themselves to be quite accurate in practice, allowing the Monte Carlo practitioner to easily estimate the collision probability between two particles. In turn, this will allow us to compute the annihilation rate in positronic systems, therefore presenting the chance to directly compare with the experimental results.

In order to show that this is exactly the case, in the next section we present the results obtained computing $\langle\delta(r_{-+})\rangle$ for some model systems whose exact values are easily obtained using different methods.

Methods similar to ours, although quite different in many details, have been applied by Ortiz[28] and by Mairí Fraser[29] to the case of a positron embedded in the jellium. Their methods were somehow tailored to the specific system under study, so that no direct comparison with our proposals can be made. Nevertheless, the results they extracted from the simulations can be useful to seek possible correlations between the magnitude of the pileup effect and the local electron density.

III. TEST OF THE METHODS USING MODEL SYSTEMS

To test the accuracy of the proposed methods, we computed the $\langle\delta(r_{-+})\rangle$ expectation value for simple model systems containing only one electron and one positron. More specifically, some model wave functions Ψ_i were chosen in order to represent the variety of electron, positron, and electron–positron distributions that could be found in a positron atomic system. Then, the Ψ_i^2's were sampled by means of VMC simulations similar to the one discussed above, in order to collect the electron–positron distribution Ω.

We selected three model systems as representative of a fairly large class of positron complexes. The first one is given by the wave function Ψ_1 [see Eq. (8)]. The second has the analytical wave function

$$\Psi_2(\mathbf{r}_-,\mathbf{r}_+)=\exp\left[-r_-+\frac{0.15r_+-0.5r_+^2}{1+r_+}-0.5r_{-+}\right], \qquad (10)$$

where the simple exponential in r_+ of Ψ_1 is substituted by a Padé–Jastrow type, and the exact cusp condition between electron and positron has been introduced.

To mimic the presence of core and valence shells, we chose as a third function

$$\Psi_3(\mathbf{r}_-,\mathbf{r}_+)=\left\{\exp\left[-\frac{r_-+2r_-^2}{1+r_-}\right]\right.$$
$$+0.001\exp\left[\frac{15r_--3r_-^2}{1+r_-}\right]\right\}$$
$$\times\exp\left[\frac{0.15r_+-0.5r_+^2}{1+r_+}-0.5r_{-+}\right]. \qquad (11)$$

To compute the exact value $\langle\delta(r_{-+})\rangle$ for these models, we used its definition

$$\langle\delta(r_{-+})\rangle=\frac{\int\Psi_i^2(\mathbf{r}_-,\mathbf{r}_+)\delta(r_{-+})d\mathbf{r}_+\,d\mathbf{r}_-}{\int\Psi_i^2(\mathbf{r}_-,\mathbf{r}_+)d\mathbf{r}_+\,d\mathbf{r}_-}$$
$$=\frac{\int\Psi_i^2(\mathbf{r}_-,\mathbf{r}_-)d\mathbf{r}_-}{\int\Psi_i^2(\mathbf{r}_-,\mathbf{r}_+)d\mathbf{r}_+\,d\mathbf{r}_-}. \qquad (12)$$

TABLE I. $\langle \delta(r_{-+}) \rangle$ expectation values for the three model systems Ψ_1, Ψ_2, and Ψ_3. The "exact" values are computed by Eq. (12). $\langle \delta(r_{-+}) \rangle_{Pade'}$ are computed fitting Eq. (9) to the sampled distribution as explained in the text. γ is the width of the Gaussian used to compute $\langle G(r_{-+}, \gamma) \rangle$.

	$\langle \delta(r_{-+}) \rangle_{exact}$	$\langle \delta(r_{-+}) \rangle_{Pade'}$	γ	$\langle G(r_{-+}, \gamma) \rangle$
Ψ_1			0.0100	0.0216(1)
			0.0033	0.0219(1)
			0.0020	0.0222(2)
			0.0010	0.0223(3)
	0.022 602(7)	0.02229	0.0000	0.0228(3)
Ψ_2			0.0100	0.0979(2)
			0.0033	0.1028(3)
			0.0020	0.1043(4)
			0.0010	0.1058(7)
	0.109 81(1)	0.11052	0.0000	0.1095(7)
Ψ_3			0.0100	0.0842(2)
			0.0033	0.0886(3)
			0.0020	0.0901(4)
			0.0010	0.0916(7)
	0.093 99(1)	0.09382	0.0000	0.0950(7)

The simple radial integral in the numerator was computed by numerical integration on a grid, while the denominator was estimated by means of Eq. (3) using $g(\mathbf{r}_-, \mathbf{r}_+) = A^3 B^3 \times \exp[-2Ar_+ - 2Br_-]/\pi^2$.

The two distributions sampled as a function of r from Ψ_2 and Ψ_3 turned out to possess a behavior quite similar to Ψ_1. Therefore, we avoid showing all of them and refer to Fig. 1 as a template for such distributions. Due to their smoothness, we fitted them using Eq. (9) over the range 0.3–10 bohr constraining the Padé–Jastrow form to have the exact cusp condition, i.e., -0.5, -1.0, and -1.0, for the three Ψ_i, respectively. To test the correctness of the chosen fitting range, we slightly modified the lower limit without finding statistically meaningful differences. Then, the fitted ω was used to estimate both $\Omega(0)$ and the denominator in Eq. (7) by means of numerical integration. The computed results, shown as $\langle \delta(r_{-+}) \rangle_{Pade'}$, are presented in Table I together with the "exact" values computed using Eq. (12).

During the simulations we also computed the mean values $\langle G(r_{-+}, \gamma) \rangle$, where $G(r_{-+}, \gamma) = N_\gamma \exp[-r_{-+}^2/\gamma]$ is a normalized Gaussian function, for $\gamma = 0.01$, 0.0033, 0.002, and 0.001. This technique was proposed by Kenny et al.[30] and successively applied in Refs. 9 and 11. The $\langle G(r_{-+}, \gamma) \rangle$ values were extrapolated to $\gamma = 0$ by fitting them with the simple function $a\sqrt{\gamma} + b$, the extrapolation law deduced in Ref. 11 using model systems. The fitting was quite accurate for all three cases, and the results for $b = \langle G(r_{-+}, 0) \rangle$ are also shown in Table I.

Comparing $\langle \delta(r_{-+}) \rangle_{Pade'}$ with the exact results, it strikes a very good agreement between these two sets of values, the relative error being 1% at most for all the models. It must be pointed out that this level of relative accuracy is sufficient to thoroughly compare with the experimental data. It is also noted that the application to other model systems gave a similar or better relative accuracy, therefore showing the wide applicability of the method.

As already pointed out,[8,9] the extrapolated $\langle G(r_{-+}, 0) \rangle$ values are also in good agreement with the exact results. Nevertheless, one should expect to obtain really inaccurate

approximations to the exact results using $\langle G(r_{-+}, \gamma) \rangle$ with γ smaller than some threshold value. This simple idea is based on the incorrect sampling of the density close to $r = 0$ shown in Fig. 1, so the good agreement found in this and previous works calls for an explanation. This is easily obtained superimposing $G(r_{-+}, \gamma) r_{-+}^2$ to the sampled $\Omega(r_{-+})$, i.e., comparing the behavior of the two factors that form the function whose integrals must be estimated. It turns out that $G(r_{-+}, \gamma) r_{-+}^2$ for $\gamma \geq 0.001$ has its largest values where $\Omega(r_{-+})$ still behaves correctly, therefore allowing a correct estimate of the integrals. Tests carried out using smaller values of γ gave much worse results than the ones reported, so we believe it is safer to limit the values of this parameter to the range 0.001–0.01 in order to obtain a meaningful extrapolation. Although this may look problematic in some way due to the aforementioned difficulties, from the results in Table I $\langle G(r_{-+}, 0) \rangle$ appears to be a good first estimate of the exact $\langle \delta(r_{-+}) \rangle$. In conclusion, we suggest Monte Carlo practitioners always carry out both estimations, i.e., extrapolating $\langle G(r_{-+}, \gamma) \rangle$ and fitting the sampled Ω, as a way to safely estimate $\langle \delta(r_{-+}) \rangle$.

As far as diffusion Monte Carlo and the exact sampling of Ψ_0^2 are concerned, the application of these methods is straightforward, and no more complications are expected than in the VMC case.

IV. THE e$^+$LiH SYSTEM

Having verified the accuracy of the proposed method in computing Dirac's delta mean values, we applied it to the calculation of the annihilation rate $\Gamma_{2\gamma}$ of e$^+$LiH for various internuclear distances R.

Although this system has already been carefully studied employing both QMC methods[11,31] and explicitly correlated Gaussian (ECG) functions,[6,7,32] a description of $\Gamma_{2\gamma}$ as a function of the molecular geometry is still lacking. Up to now, there are only $\langle \delta(r_{-+}) \rangle = \langle \delta(r_{1+}) \rangle + \langle \delta(r_{2+}) \rangle + \langle \delta(r_{3+}) \rangle + \langle \delta(r_{4+}) \rangle$ results at $R = 3.015$ bohr $[0.0240(8)$ from DMC simulations [11] and 0.024 992 form ECG calculations [6]], at the estimated equilibrium distance $R = 3.348$ bohr $(0.027\,252)$,[7] and the nonadiabatic results of Mitroy and Ryzhikh, 0.034 016 and 0.032 588.[32] These last values were obtained using ECG in connection, respectively, with the stochastic variational minimization (SVM) and the frozen-core SVM (FCSVM) methods, and are roughly 15%–20% larger than the ECG[6,7] and DMC[11] clamped-nuclei ones. This unexpected result led Strasburger[6] to consider the possibility of the flattening of the potential energy curve of e$^+$LiH with respect to the LiH one, a feature that may allow the positronic molecule to visit the large internuclear distance region where the Dirac's delta mean value is expected to be larger. However, Mitroy and Ryzhikh[32] pointed out that simple ECGs may not represent the best basis functions to describe vibrational nuclear motion, and that their vibrational averaged nuclear distances are probably too large.

In a previous work,[31] we computed the complete curve using the DMC technique, showing that the flattening is indeed present, and that a strong redshift of the vibrational spectrum with respect to LiH must be expected. Unfortu-

nately, due to the high computational cost of our highly correlated trial wave functions, at that time we did not compute the behavior of $\langle \delta \rangle$ as a function of R. In this work we still adopt the Born–Oppenheimer (BO) approximation, so we predict the annihilation rate for each vibrational state of the system and compare our values with the nonadiabatic results of Mitroy and Ryzhikh.[32]

In order to study the effect of the molecular geometry on the annihilation rate without using the computationally expensive wave function used in Ref. 11, we decided to employ a model potential approach to eliminate the "core" electrons of the Li^+ fragment. We believe such an approach to be physically well grounded, as explained by the following supporting reasons. First, the ECG calculations carried out by Strasburger[6,7] on the e^+LiH system show that the annihilation takes place primarily with the two electrons that may be attributed to the H^- fragment. Second, the frozen core approximation developed by Mitroy and Ryzhikh[4] has been found to describe accurately the annihilation process in e^+Li, e^+Be, $LiPs$, and $e^+He\,^3S$ when compared with the corresponding all-electron calculations.

In order to reduce the number of active electrons, we used for e^+LiH the model Hamiltonian

$$\mathcal{H}_{mod} = -\frac{1}{2}[\nabla_1^2 + \nabla_2^2 + \nabla_+^2] + V_{mod}^e(\mathbf{r}_1) + V_{mod}^e(\mathbf{r}_2) - \frac{1}{r_{H1}}$$
$$-\frac{1}{r_{H2}} + \frac{1}{r_{12}} + \frac{1}{r_{H+}} - \frac{1}{r_{1+}} - \frac{1}{r_{2+}} + V_{mod}^+(\mathbf{r}_+).$$
(13)

Here, the r_{ij} are interparticle distances, 1 and 2 being the electrons, $+$ the positron, and H the hydrogen nucleus. Moreover, the Bardsley's model potential[33]

$$V_{mod}^e(\mathbf{r}_i) = \frac{-1 + 10\exp[-2.202r_{iLi}]}{r_{iLi}},$$
(14)

where r_{iLi} is the distance between the ith electron and the Li nucleus, has been used to represent the $1s^2$ Li^+ core electrons. To model the interaction of the positron with the frozen Li^+ fragment, we simply added to the repulsive Coulomb potential of the nucleus the potential of the two frozen core electrons as described by an $STO-1s$ orbital with $Z=3$, obtaining

$$V_{mod}^+(\mathbf{r}_+) = \frac{3}{r_{Li+}} + 6\exp[-6r_{Li+}]$$
$$-2\frac{1-\exp[-6r_{Li+}]}{r_{Li+}},$$
(15)

where r_{Li+} is the Li–positron distance.

To test the accuracy of this model potential, we computed the energy for the ground state of the three systems Li, Li^-, and LiPs. The energy values are, respectively, $-0.1953(2)$ hartree, $-0.2191(3)$ hartree, and $-0.4485(3)$ hartree. They give an electron affinity of $0.0238(4)$ hartree, a positron affinity (PA) of $0.2294(4)$ hartree, and a Ps binding energy (BE) of $0.0032(4)$ hartree. While the electron affinity turns out to be in fair agreement with the experimental value, namely 0.023 hartree,[34] both PA and BE are roughly 0.009

hartree smaller than the best estimate.[4] These discrepancies might be due to the absence of polarization effects of the core electrons due to the two active electrons and the positron, and to a relatively inaccurate representation of the $1s^2$ electron density by means of a single $STO-1s$ function. Nevertheless, since we are primarily interested in obtaining a semiquantitative description of the changes in $\Gamma_{2\gamma}$ for this system, we believe the approximations introduced in the model Hamiltonian to be small enough to allow for a correct prediction of the trend for this important observable.

In order to accurately describe the wave function of the three active particles at the VMC level, we employed a trial wave function form similar to the one used in Ref. 11, but slightly modified to include the polarization of the electron and positron density of the PsH fragment due to the Li^+ potential. Specifically, the analytical form in Eq. (7) of Ref. 11 has been multiplied by a Padé–Jastrow factor depending on the z coordinate of each particle: the z axis was chosen as the LiH bond axis, the H nucleus being located at the origin and the Li on the negative z axis. The wave function parameters were fully optimized for every nuclear distance R minimizing the variance of the local energy over a fixed sample of configurations.[35,36] This procedure is already well described in the literature,[13] so we will skip unnecessary details. The ensemble of walkers used in the optimization was generated by DMC simulations in order to bias the walkers' distribution towards the exact density. Usually, four or five optimization steps were carried out for each R.

We started the optimization process of the wave function at $R=20$.[11] At the end of the optimization procedure, R was decreased and the wave function reoptimized for the new distance. This procedure gives the chance to monitor the changes of the wave function with R, but might increase the possibility of remaining stuck in a local minimum in the parameter space during the optimization.

Having optimized at VMC level the approximate wave functions for various distances, these were employed in long DMC simulations to project the remaining excited-state contributions and to compute more accurate mixed expectation values. For all the simulations, a time step of 0.005 hartree^{-1} was used, together with a population of 9000 walkers. These two simulation parameters were found adequate to make statistically negligible both the time-step bias and the population effect in the DMC simulations.

The DMC results for the energy and for the $\langle \delta(r_{-+})\rangle$ of this model system are shown in Table II. There, the energy values represent the ground-state energy of the model Hamiltonian Eq. (13), $\langle \delta(r_{-+})\rangle_{Pade'}$ are the total collision probabilities estimated using the electron–positron distribution, i.e., $\langle \delta(r_{1+})\rangle + \langle \delta(r_{2+})\rangle$, while $\langle G(r_{-+},0)\rangle$ are the extrapolated Gaussian values. Here, the electron–positron distributions were fitted with the function in Eq. (9), constraining its cusp to be $-0.5 + cusp(\Psi_T)$.

The energy values obtained in Ref. 31, after having subtracted the repulsion $1/R$ between the H nucleus and the Li^+ core and the total energy of the Li^+ fragment ($-7.279\,913$ hartree[3]) to estimate the leptonic energy of the PsH moiety, are shown in Fig. 2 together with the DMC results obtained in this work.

TABLE II. Lepton energies, $\langle \delta(r_{-+}) \rangle_{\text{Pade}'}$, and $\langle G(r_{-+},0) \rangle$ mean values for the e^+LiH model system. All quantities in atomic units.
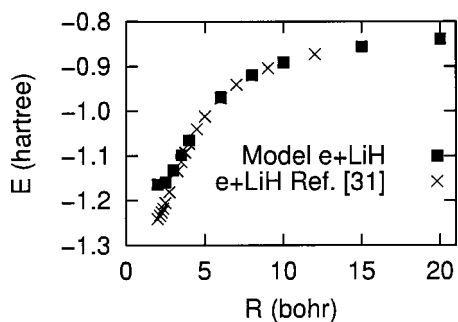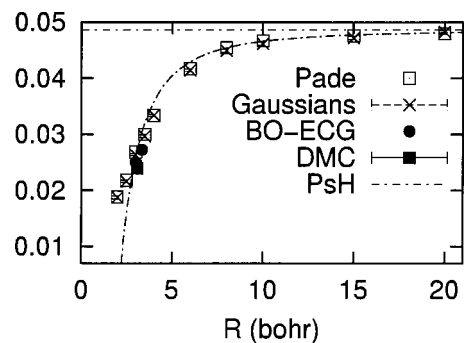
R	$\langle E \rangle$	$\langle \delta(r_{-+}) \rangle_{\text{Pade}'}$	$\langle G(r_{-+},0) \rangle$
2.0	−1.164 37(9)	0.018 84	0.0182(2)
2.5	−1.159 36(7)	0.021 78	0.0210(2)
3.0	−1.131 96(6)	0.026 84	0.0256(2)
3.5	−1.097 98(5)	0.030 00	0.0288(2)
4.0	−1.064 85(5)	0.033 34	0.0324(2)
6.0	−0.969 85(4)	0.041 66	0.0402(2)
8.0	−0.919 95(3)	0.045 44	0.0436(3)
10.0	−0.891 60(3)	0.046 66	0.0448(3)
15.0	−0.856 34(2)	0.047 54	0.0458(3)
20.0	−0.839 32(2)	0.047 94	0.0468(3)
∞	−0.789 18(1)	0.048 60	0.0484(3)

FIG. 3. Computed $\langle \delta \rangle$ results for e^+LiH system at various internuclear distances.

For $R \geq 4$, the results from the model system follow closely the more accurate all-electron FN-DMC values, showing that the model potential correctly describes the polarization of PsH due to the interaction with Li$^+$. For shorter distances the approximation of considering Li$^+$ frozen is no longer accurate, so that a discrepancy between the two sets of results is expected. It is also important to remember that the Bardsley's potential was tailored only to describe the atom in its ground-and valence excited states, not to describe bonds correctly in molecules.

Figure 3 shows the two computed $\langle \delta(r_{-+}) \rangle$ values as a function of the internuclear distance R, together with the ECG results of Strasburger [6,7] and the DMC result of Ref. 11. The latter results can be used to evaluate the total accuracy of our computed collision probabilities.

From Fig. 3 it is clear that both the $\langle \delta(r_{-+}) \rangle_{\text{Pade}'}$ and the $\langle G(r_{-+},0) \rangle$ are in good agreement, the second differing from the first by at most two standard deviations. This allows us to believe that we are accurately estimating the mixed distribution mean value obtained by the standard DMC technique. Improved results could be obtained only by sampling Ψ_0^2.
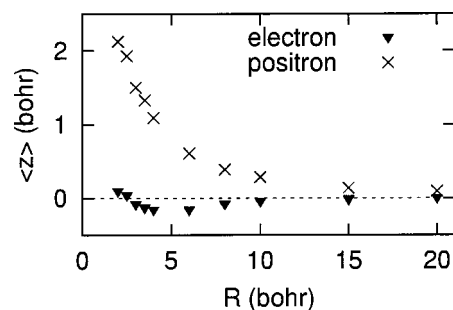
As far as the total accuracy is concerned, at $R = 3.015$ bohr both all-electron ECG[6,7] and DMC results[11] appear to be smaller than the model ones by roughly 7%. Instead, on going towards large R the mean value seems to correctly converge to the very accurate ECG value, namely $\langle \delta(r_{-+}) \rangle_{\text{PsH}} = 0.048\,74$,[3] and to the new DMC 0.0486 estimate carried out in this work using the electron–positron distribution. From this comparison, one could expect our es-

timation to slightly degrade going towards small R, without becoming embarrassingly inaccurate to create concerns about the usefulness of this model system.

The overall trend of the collision probability shows a net decrease going towards short R, a feature already suggested by Mitroy and Ryzhikh.[32] This can be easily understood remembering that the Li$^+$ model potential repels the positron, while attracting the two electrons. It is not easy to infer any possible analytical model to describe these joined effects, although for large R one could propose a limiting $1/R^2$ form due to the polarization of the two distributions by the electric field of Li$^+$. We show in the Appendix that this reasoning is indeed correct for any observable by means of first-order perturbation theory. "Experimental" evidence that this is the case is given by the fairly good fitting of the $\langle \delta \rangle$ results at $R = 10$, 15, and 20 bohr with the simple form $0.0486 + b/R^2$, where $b = -0.204\,48$.

Various other mean values were computed during the DMC simulations in order to obtain some physical insight on the electron and positron density behavior. Figure 4 reports the mean value of the z coordinate for the two particles giving information on the polarization of the two lepton densities. It is clear that the positronic distribution is polarized by the model potential in the direction opposite to the electronic one. Moreover, it appears to be more easily polarized than the electronic one always showing larger $\langle z \rangle$ values. This fact can be easily explained by noticing that the positron distribution is more diffuse than the electron one, so that it is more strongly repelled by the electric field. Interestingly, at $R = 2$ and 2.5 bohr the electron distribution reverses its polarization, showing $\langle z \rangle > 0$. We believe this effect is due to the

FIG. 2. Energy of the PsH moiety computed from Eq. (13) and from the e^+LiH results of Ref. 31 as explained in the text.

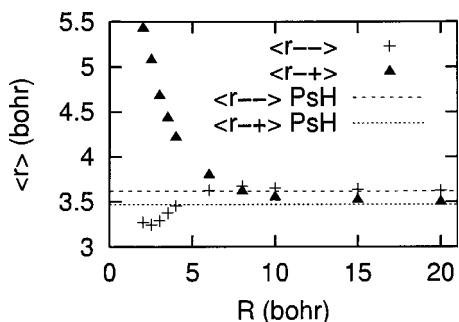FIG. 4. Electron and positron mean value of the z coordinate as a function of the internuclear distance.

FIG. 5. Electron–electron and electron–positron mean distances as function of the internuclear distance.

TABLE III. Vibrational state energy $\langle E \rangle_\nu$, averaged $\langle \delta(r_{-+}) \rangle_\nu$ and $\langle R \rangle_\nu$ values for the e^+LiH model system. All quantities in atomic units.

ν	$\langle E \rangle_\nu$	$\langle \delta \rangle_\nu$	$\langle R \rangle_\nu$
0	−8.105	0.0295	3.423
1	−8.102	0.0305	3.571
2	−8.098	0.0315	3.732
3	−8.095	0.0325	3.906
4	−8.092	0.0334	4.094
5	−8.089	0.0344	4.294
6	−8.087	0.0352	4.503
7	−8.085	0.0361	4.718
8	−8.083	0.0369	4.938
9	−8.081	0.0376	5.166
10	−8.079	0.0383	5.408
11	−8.077	0.0390	5.675
12	−8.076	0.0397	5.985
13	−8.074	0.0405	6.356
14	−8.073	0.0414	6.803
15	−8.072	0.0421	7.243

repulsive region of the Li$^+$ core potential that pushes away the electrons for such small nuclear distances, therefore modeling the exchange effect created by an antisymmetric wave function.

Figure 5 shows the average values for the electron–electron and electron–positron distances. While the electron–positron mean distance $\langle r_{-+} \rangle$ increases monotonically upon decreasing R, the electron–electron distance $\langle r_{--} \rangle$ shows a shallow maximum around $R = 8$ bohr and a deep minimum around $R = 2.5$ bohr. We believe the maximum is due to the competition between the positron and the Li$^+$ model potential to bind an electron. More specifically, although polarized towards positive z, the positron still attracts one of the two electrons to form the Ps subcluster, increasing the distance from the second electron that is free to be polarized in the direction of the Li$^+$ core. On going towards smaller R, the positron is pushed far out the bond region, losing its ability to polarize the electrons that are now both strongly attracted by the model potential. This interaction leads them to move in the small volume between H and Li$^+$, therefore decreasing their mean distance. Then, for R smaller than 2.5 bohr, the electron–core repulsion pushes the electrons out from the bond region, with the net effect of increasing their mean distance. This effect has also been observed by plotting the intracule electron distributions obtained during the DMC simulations.

It is worth mentioning that similar conclusions can be drawn analysing the VMC results obtained as a by-product of the optimization stages.

Having studied the overall behavior of $\langle \delta \rangle$, $\langle z \rangle$, and $\langle r \rangle$, we now turn to compute the vibrationally averaged annihilation probabilities. To obtain these quantities, we interpolated our $\langle \delta \rangle$ results by means of the analytical form $\Delta(R) = 0.0486 - 2aR/(1 + bR + cR^2 + dR^3)$. The fitted parameters are $a = 1.059\,45$, $b = 97.5779$, $c = -37.9705$, and $d = 12.2715$. Then, the potential energy curve of e^+LiH obtained in Ref. 31 was fitted with the modified Morse potential

$$V_M(R) = -8.0699 + A\{1 - \exp[-B(R-C)]\}^2 - A$$
$$- D\{1 - \exp[-(R/F)]^6\}/(2R^4), \quad (16)$$

obtaining $A = 0.034\,44$ hartree, $B = 0.720\,30$ bohr^{-1}, $C = 3.3060$ bohr, $D = 21.1796$ bohr^{-3}, and $F = 5.882\,17$ bohr. The last term in Eq. (16) has been introduced in order to

correctly represent the charge-induced dipole interaction between Li$^+$ and PsH. The nuclear Schrödinger equation for this potential was then solved using the grid method proposed by Tobin and Hinze,[37] and the numerical wave functions $\phi_\nu(\mathbf{R})$ were then used to compute vibrationally averaged mean values for zero total angular momentum. More specifically, we computed

$$\langle O \rangle_\nu = \frac{\int d\mathbf{R}\, \phi_\nu^2(R) O(R)}{\int d\mathbf{R}\, \phi_\nu^2(R)}, \quad (17)$$

where $O(R)$ is $\Delta(R)$ or any other function of R.

In Table III we show the results for $\langle E \rangle_\nu$, $\langle \delta \rangle_\nu$, and $\langle R \rangle_\nu$ computed over the first 16 bound vibrational states. The $\langle \delta \rangle_\nu$ values increase in an almost linear fashion going towards large ν, as expected by the steady increase of $\langle R \rangle_\nu$ due to the vibrational excitation. Comparing $\langle \delta \rangle_0 = 0.0295$ with the value of $\Delta(R)$ at the equilibrium distance of our fitted potential, namely 0.0291 at 3.353 bohr, it appears that the ground level vibrational motion only slightly increases the probability of collision between the electrons and the positron with respect to the one at the equilibrium distance. This finding is in line with the small difference between the equilibrium distance and the average nuclear distance $R_0 = 3.42$ bohr. We relate these outcomes to the almost linear behavior of $\Delta(R)$, and to the shape of $R^2 \phi_0^2(R)$ in the region around the potential minimum, where it resembles a Gaussian. Here, we stress that the shorter equilibrium distance obtained in this work (3.353 bohr), with respect to the one obtained in Ref. 31 (3.458 bohr), is just a side effect of the fitting process and of the analytical form in Eq. (16). In turn, this means that the energies for the vibrational states could be, and indeed are, slightly different from the ones published in Ref. 31, which we believe to be more accurate.

Although our vibrationally averaged result for $\nu = 0$ $\langle \delta \rangle_0 = 0.0295$ appears to be roughly 8% larger than the ECG result (0.027 252) at the equilibrium distance 3.348 bohr,[7] suggesting a fairly large effect of the nuclear motion, we believe this outcome is primarily due to the 7% larger collision probabilities computed using our model system. These

two evidences seem to rule out Strasburger's suggestion[6] of a large increase of the collision probability due to the quantum nuclear motion for the $\nu = 0$ state. They indicate that approximating the averaged collision probability for the vibrational ground state simply by using its value at the equilibrium distance could be a fairly accurate procedure. Moreover, these conclusions agree with Mitroy and Ryzhikh's[32] warnings that both the SVM and FCSVM results, although proving the overall stability of e$^+$LiH, are not well converged to the exact ones. For instance, their $\langle R \rangle_0$ values, respectively, 4.182 and 3.964 bohr, are larger than the minimum of the ECG and DMC potential curves by more than 0.5 bohr. This discrepancy cannot be accounted for by the zero-point motion of the positron complex. These larger distances between the two fragments Li$^+$ and PsH in the nonadiabatic treatment imply a reduced distortion of the lepton densities of PsH with respect to the one at the Born–Oppenheimer equilibrium, and therefore too large an annihilation rate. However, it is interesting to notice that both FCSVM (0.032 588) and SVM (0.034 016)[32] collision probabilities are really close to our Born–Oppenheimer one at $R = 4.0$ bohr. In our view, this agreement stresses, again, the importance of the local electric field in defining the collision probability and the overall accuracy of the SVM approach in describing the relative densities in a positronic complex.

As far as the behavior of $\langle \delta(R) \rangle_\nu$ is concerned, the steady increase on going towards large ν indicates that the annihilation rate does depend on the quantum vibrational state of the molecule. Although the trend of these results could be specific to the e$^+$LiH system and perhaps of other polar molecules as well, it strongly indicates that any theory formulated to describe "on the fly" annihilation of e$^+$ due to Feshbach resonances must include this effect in order to go beyond "order of magnitude comparison"[38] and to predict accurately the annihilation rate. In our view, this opens a new avenue of exploration in positron physical chemistry where the understanding of the vibrational motion effect on positron annihilation by molecular systems is of prime importance.

V. CONCLUSIONS

In this work we have critically compared methods that may be useful to compute the annihilation rate in positronic systems in the framework of the QMC methods. Moreover, we have presented a simple, but nevertheless solid and accurate, method based only on the interparticle distribution sampling. After having tested it using model systems, we employed the method to compute $\langle \delta(r_{-+}) \rangle$ for e$^+$LiH for several internuclear distances. These results allowed us to discuss many interesting features of this positronic complex, and to predict that the annihilation probability increases upon increasing the vibrational quantum number ν. We notice that a similar behavior of $\langle \delta(r_{-+}) \rangle$ may be expected also for e$^+$LiF due to the polarization of the positronic density of the PsF fragment by the Li$^+$ core. The situation could be quite different for the e$^+$BeO case where the positron density is expected to be centered on Be at large nuclear distances (the two fragments e$^+$Be and O have lower total energy than Be$^+$ and PsO[39]), and to move on the O side of the molecule when

the distance decreases. This effect is due to the electron transfer from Be to O that creates the large molecular dipole moment. From our experience on these systems we expect $\langle \delta(r_{-+}) \rangle$ for e$^+$Be to be smaller than the one for the polar molecule, so the vibrationally excited states close to the dissociation threshold may have smaller annihilation rates than the ground vibrational state.

It is also interesting to speculate on the behavior of the annihilation rate versus the vibrational quantum number for other simple systems like e$^+$Li$_2$ and e$^+$Be$_2$. Here, the symmetry of the systems can play an important role in defining the annihilation rate. For instance, decreasing the nuclear distance one may expect to find the positron localized between the two atomic fragments due to its ability to polarize the two atomic electron densities: in this situation the annihilation rate could be quite different from the atomic one. Although it is easy to infer the existence of a bound state for these complexes at large nuclear distances employing the basic valence bond resonance idea

$$e^+ A_1 + A_2 \leftrightarrow A_1 + e^+ A_2, \tag{18}$$
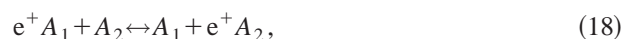
it still remains to demonstrate the stability of these systems for nuclear distances close to the equilibrium geometry of the neutral parent molecules.

As a rule of thumb to predict the stability of a nonpolar molecule, one can use the adiabatic ionization potential (AIP) as proposed by Mitroy et al.[40] For the $X^1\Sigma_g^+$ ground state of Li$_2$ the experimental AIP is 0.189 hartree,[41] slightly lower than the atomic one, 0.198 14 hartree.[42] Also, for the $X^1\Sigma_g^+$ ground state of Be$_2$, one might expect a similar lowering of the AIP with respect to the atomic one, 0.343 hartree,[42] so that a value of around 0.335 hartree could be regarded as a safe upper bound to the true AIP. Both these values fall inside the upper and lower I.P. limits for positron binding obtained by Mitroy et al.[40] for one- and two-valence electron atoms, therefore suggesting that the two complexes should be stable. We understand that this model is just a rough approximation for our molecular systems.[43] Nevertheless, a positron bound to an atom or a molecule is always characterized by a quite diffuse density. This allows one to neglect some of the real features of the electron density close to the nuclei as a first approximation, and focus only on the asymptotic properties of the electron cloud that are correlated to the I.P. and to the polarizability.

As far as Be$_2$ is concerned, the AIP larger than the Ps binding energy (0.25 hartree) suggests a mechanism based on the electron cloud polarization as responsible for the binding. Moreover, the lowering of the AIP with respect to the atomic one, and the large polarizability of this molecule (roughly twice the atomic one) seem to indicate its ability to form a stronger bond with the positron than the Be atom alone.[4] Conversely, Li$_2$ has an AIP smaller than the Ps binding energy, suggesting that the polarization of the Ps cluster may be held responsible for the positron binding. However, Li is close to the lower stability threshold of the positron–atom complexes, and we do not feel confident in proposing the stability of the molecular complex with respect to the Ps + Li$_2^+$ dissociation pathway.

J. Chem. Phys., Vol. 116, No. 7, 15 February 2002

Positronic systems   2861

Right now, QMC methods are the best-suited computational techniques to carry out such a study since six- and eight-electron systems are too large to be studied with ECGs unless the frozen core approximation is used. With the addition to the QMC "bag of tricks" of a robust method for computing annihilation rates, such a study could become routine in molecular physical chemistry, allowing the exploration of many interesting features of these "exotic" compounds.

Moreover, many more other technically oriented applications could be devised. Positronium annihilation in polymers and membranes, positron annihilation in silicon nanocluster, nanodevices, fullerenes, and carbon nanotubes are just a few that could be quite easily interpreted with the help of such a method.

Our hope is that this work will help this kind of application to blossom and to lead to a better understanding of the basic interaction schemes that a positron has with ordinary matter.

ACKNOWLEDGMENTS

APPENDIX: FIRST-ORDER PERTURBATION THEORY OF EXPECTATION VALUE

In this Appendix we show that the correction to the expectation value of every observable O for PsH interacting with the Li^+ core follows the limiting analytical form R^{-2} for large R. This is indeed a general result for positronic atom systems immersed in a weak electric field. From perturbation theory one can write the first-order corrected wave function for the ground state as

$$\Psi_0^{(1)} = \Psi_0^{(0)} + \sum_{i \neq 0} \frac{\int \Psi_i^0 V \Psi_0^{(0)} d\mathbf{R}}{E_0^{(0)} - E_i^{(0)}} \Psi_i^{(0)}$$

$$= \Psi_0^{(0)} + \sum_{i \neq 0} c_i^{(0)} \Psi_i^{(0)}, \tag{A1}$$

where $\Psi_i^{(0)}$ are the eigenstates of the unperturbed Hamiltonian (i.e., the PsH), $E_i^{(0)}$ its eigenvalues, and V the perturbation potential. The expectation value of the observable O can be computed using

$$\langle O \rangle = \frac{\mathbf{c}^t \mathbf{O} \mathbf{c}}{\mathbf{c}^t \mathbf{I} \mathbf{c}}, \tag{A2}$$

where $\mathbf{O}_{ji} = \int \Psi_j^{(0)} O \Psi_i^{(0)} d\mathbf{R}$, while $\mathbf{c} = \{1, c_1^{(0)}, c_2^{(0)}, \ldots\}$. If the perturbation potential is small with respect to the total energy, then $c_i^{(0)} \ll 1$ and $\mathbf{c}^t \mathbf{I} \mathbf{c} = 1 + \sum_{i \neq 0} (c_i^{(0)})^2 \simeq 1$. This fact allows the introduction of a further approximation into Eq. (A2),

$$\langle O \rangle \simeq \mathbf{c}^t \mathbf{O} \mathbf{c} = \langle O \rangle_{00} + 2 \sum_{i \neq 0} c_i^{(0)} \langle O \rangle_{0i} + \sum_{i,j \neq 0} c_j^{(0)} c_i^{(0)} \langle O \rangle_{ji}$$

$$\simeq \langle O \rangle_{00} + 2 \sum_{i \neq 0} c_i^{(0)} \langle O \rangle_{0i}, \tag{A3}$$

showing that the first-order change in the expectation value $\langle O \rangle$ is linearly dependent on the $c_i^{(0)}$'s.

For our specific case, namely PsH interacting with the Coulomb potential of Li^+ at distance R, for $R \to \infty$ the perturbing interaction potential can be written as

$$V = \sum_k \frac{q_k}{R_{q_k Li}} \simeq \sum_k q_k \left(\frac{1}{R} - \frac{z_k}{R^2} \right), \tag{A4}$$

where the molecular geometry is as in the main text, while q_k are the leptonic charges. This approximation is equal to consider the electron and positron densities constant in a plane parallel to the xy plane. Introducing this approximation in the integrals in Eq. (A1), one gets

$$\int \Psi_i^{(0)} V \Psi_0^{(0)} d\mathbf{R} \simeq \sum_k q_k \frac{1}{R} \int \Psi_i^{(0)} \Psi_0^{(0)} d\mathbf{R}$$

$$+ \sum_k q_k \int \Psi_i^{(0)} \frac{z_k}{R^2} \Psi_0^{(0)} d\mathbf{R}$$

$$= \frac{\sum_k q_k \int \Psi_i^{(0)} z_k \Psi_0^{(0)} d\mathbf{R}}{R^2}. \tag{A5}$$

This result shows that the c_i in Eqs. (A2) and (A3) are proportional to $1/R^2$, therefore proving that this is also the analytical form of the leading correction to the unperturbed ground-state expectation values $\mathbf{O}_{00}$.

[1] O. E. Mogensen, *Positron Annihilation in Chemistry* (Springer, Berlin, 1995).
[2] R. Krause-Rehberg and H. S. Leipner, *Positron Annihilation in Semiconductors* (Springer, Berlin, 1999).
[3] G. G. Ryzhikh, J. Mitroy, and K. Varga, J. Phys. B **31**, 3965 (1998).
[4] J. Mitroy and G. G. Ryzhikh, J. Phys. B **34**, 2001 (2001).
[5] N. Jiang and D. M. Schrader, J. Chem. Phys. **109**, 9430 (1998).
[6] K. Strasburger, J. Chem. Phys. **111**, 10555 (1999).
[7] K. Strasburger, J. Chem. Phys. **114**, 615 (2001).
[8] D. Bressanini, M. Mella, and G. Morosi, Phys. Rev. A **55**, 200 (1997).
[9] D. Bressanini, M. Mella, and G. Morosi, Chem. Phys. Lett. **272**, 370 (1997).
[10] D. Bressanini, M. Mella, and G. Morosi, Phys. Rev. A **57**, 1678 (1998).
[11] M. Mella, G. Morosi, and D. Bressanini, J. Chem. Phys. **111**, 108 (1999).
[12] M. W. J. Bromley, J. Mitroy, and G. G. Ryzhikh, Nucl. Instrum. Methods Phys. Res. B **171**, 47 (2000).
[13] B. L. Hammond, W. A. Lester, Jr., and P. J. Reynolds, *Monte Carlo Methods in Ab Initio Quantum Chemistry*, 1st ed. (World Scientific, Singapore, 1994).
[14] P. Langfelder, S. M. Rothstein, and J. Vrbik, J. Chem. Phys. **107**, 8525 (1997).
[15] R. Assaraf and M. Caffarel, Phys. Rev. Lett. **83**, 4682 (1999).
[16] R. Assaraf and M. Caffarel, J. Chem. Phys. **113**, 4028 (2000).
[17] S. A. Alexander and R. L. Coldwell, J. Chem. Phys. **103**, 2572 (1995).
[18] The "pileup" effect has been found by us to account at least for half of the annihilation probability of a positron bound to a molecular system.
[19] Our earlier attempts to introduce explicit correlation between the electrons and the positron did not yield any success. We believe this outcome to be primarily due to a lack of flexibility of the trial wave function that was not able to account for the relevant changes in the electronic distributions after the positron addition. Moreover, the minimization of the variance of the local energy resulted in a reduction of the positron–nuclear repulsion in-

stead of increasing the correlation between electrons and the positron.

[20] J. B. Anderson, J. Chem. Phys. **63**, 1499 (1975).

[21] J. B. Anderson, J. Chem. Phys. **65**, 4121 (1976).

[22] P. J. Reynolds, D. M. Ceperley, B. J. Alder, and W. A. Lester, Jr., J. Chem. Phys. **77**, 5593 (1982).

[23] M. Mella, D. Bressanini, and G. Morosi, Phys. Rev. A **63**, 024503 (2001).

[24] R. N. Barnett, P. J. Reynolds, and W. A. Lester, Jr., J. Comput. Phys. **96**, 258 (1991).

[25] S. Baroni and S. Moroni, Phys. Rev. Lett. **82**, 4745 (1999).

[26] C. J. Umrigar, M. P. Nightingale, and K. J. Runge, J. Chem. Phys. **99**, 2865 (1993).

[27] M. Mella (unpublished).

[28] G. Ortiz, Ph.D. thesis (Ecole Polytechnique Federale de Lausanne, 1992).

[29] M. Mairí Fraser, Ph.D. thesis (Imperial College of London, 1997).

[30] S. D. Kenny, G. Rajagopal, and R. J. Needs, Phys. Rev. A **51**, 1898 (1995).

[31] M. Mella, G. Morosi, D. Bressanini, and S. Elli, J. Chem. Phys. **113**, 6154 (2000).

[32] J. Mitroy and G. G. Ryzhikh, J. Phys. B **33**, 3495 (2000).

[33] J. N. Bardsley, Case Stud. At. Phys. **4**, 299 (1974).

[34] H. Hotop and W. C. Lineberg, J. Phys. Chem. Ref. Data **14**, 731 (1985).

[35] A. A. Frost, J. Chem. Phys. **41**, 478 (1964).

[36] H. Conroy, J. Chem. Phys. **41**, 1327 (1964).

[37] F. L. Tobin and J. Hinze, J. Chem. Phys. **63**, 1034 (1975).

[38] G. F. Gribakin, Phys. Rev. A **61**, 022720 (2000).

[39] D. Bressanini, M. Mella, and G. Morosi, J. Chem. Phys. **109**, 1716 (1998).

[40] J. Mitroy, M. W. J. Bromley, and G. Ryzhikh, J. Phys. B **32**, 2203 (1999).

[41] R. A. Bernheim, L. P. Gold, and T. Tipton, J. Chem. Phys. **78**, 3635 (1983).

[42] S. G. Lias, I. E. Bartmess, J. F. Liebman, J. L. Holmes, R. D. Levin, and W. G. Hallard, J. Phys. Chem. Ref. Data Suppl. **17**, 1 (1988).

[43] M. Mella, G. Morosi, and D. Bressanini, J. Chem. Phys. **112**, 3928 (2000).